CHAPTER 7

Uniform Sampling of Signals and Automatic Gain Control

Uniform sampling of both bandlimited lowpass signals and bandpass signals is studied in detail. The conditions for sampling a signal without aliasing are reviewed. Special scenarios relating to the IF frequency and the sampling rate are explained. Signal reconstruction as it relates to the sampling theorem is also discussed. In the context of data conversion, it is imperative to the performance of the modem to control the long-term changes in the received signal strength, thus preserving the overall dynamic range. This must be done without introducing significant clipping if the signal becomes large, or under-representation by the data converter if the signal becomes small. Either case would degrade the signal quality and would have adverse effects on the desired SNR. The automatic gain control algorithm discussed in this chapter, one of several ways of implementing gain control, serves to regulate the signal strength in order to preserve optimal performance.

This chapter is divided into four major sections. In Sections 7.1 and 7.2, the uniform sampling theorem is discussed in some detail as it relates to both lowpass and bandpass sampling. That is, uniform sampling as applied to quadrature baseband signaling as well as complex sampling at IF or RF is discussed. The AGC algorithm is considered in Section 7.3. This section also addresses the implication of the peak to average power ratio of a signal and its impact on the AGC. Section 7.4 contains the appendix.

7.1 Sampling of Lowpass Signals

The sampling theorem requires that a lowpass signal be sampled at least at twice the highest frequency component of the analog band-limited signal. This in essence ensures that the spectral replicas that occur due to sampling do not overlap and the original signal can be reconstructed from the samples with *theoretically* no distortion.

7.1.1 Signal Representation and Sampling

Given a band-limited analog lowpass signal $x_a(t)$—that is, the highest frequency component of $x_a(t)$ is strictly less than a given upper bound, say $B/2$—then $x_a(t)$ can be suitably represented by a discrete signal $x(n)$ made up of uniformly spaced samples collected at a minimum rate of B samples per second. B is known as the Nyquist rate. Inversely, given the discrete samples $x(n)$ sampled at least at the Nyquist rate, the original analog signal $x_a(t)$ can then be reconstructed without loss of information. In the remainder of this section, we will discuss the theory behind lowpass sampling.

The Fourier transform of an analog signal $x_a(t)$ is expressed as

$$X_a(F) = \int_{-\infty}^{\infty} x_a(t)e^{-j2\pi Ft}dt \tag{7.1}$$

The analog time domain signal can be recovered from $X_a(F)$ via the inverse Fourier transform as:

$$x_a(t) = \int_{-\infty}^{\infty} X_a(F)e^{j2\pi Ft}dF \tag{7.2}$$

Next, consider sampling $x_a(t)$ periodically every T_s seconds to obtain the discrete sequence:

$$x(n) = x_a(t)\Big|_{t=nT_s} \equiv x_a(nT_s) \tag{7.3}$$

The spectrum of $x(n)$ can then be obtained via the Fourier transform of discrete aperiodic signals as:

$$X(f) = \sum_{n=-\infty}^{\infty} x(n)e^{-j2\pi fn} \tag{7.4}$$

Similar to the analog case, the discrete signal can then be recovered via the inverse Fourier transform as:

$$x(n) = \int_{-1/2}^{1/2} X(f)e^{j2\pi fn}df \tag{7.5}$$

To establish a relationship between the spectra of the analog signal and that of its counterpart discrete signal, we note from (7.2) and (7.3) that:

$$x(n) = x_a(nT_s) = \int_{-\infty}^{\infty} X_a(F) e^{j2\pi \frac{F}{F_s} n} dF \tag{7.6}$$

Note that from (7.6), periodic sampling implies a relationship between analog and discrete frequency $f = F/F_s$, thus implying that when comparing (7.5) and (7.6) we obtain:

$$\int_{-1/2}^{1/2} X(f)\, e^{j2\pi fn} df \Bigg|_{\substack{f=F/F_s \\ df=dF/F_s}} = \frac{1}{F_s} \int_{-F_s/2}^{F_s/2} X\left(\frac{F}{F_s}\right) e^{j2\pi \frac{F}{F_s} n} dF = \int_{-\infty}^{\infty} X_a(F) e^{j2\pi \frac{F}{F_s} n} dF \tag{7.7}$$

The integral on the right hand side of (7.7) can be written as the infinite sum of integrals:

$$\int_{-\infty}^{\infty} X_a(F) e^{j2\pi \frac{F}{F_s} n} dF = \sum_{l=-\infty}^{\infty} \int_{(l-1/2)F_s}^{(l+1/2)F_s} X_a(F) e^{j2\pi \frac{F}{F_s} n} dF \tag{7.8}$$

Recognizing that $X_a(F)$ in the interval $((l - 1/2)F_s,(l + 1/2)F_s)$ is equivalent to $X_a(F + lF_s)$ in the interval $(-F_s/2, F_s/2_s)$, then the summation term on the right hand side of (7.8) becomes:

$$\sum_{l=-\infty}^{\infty} \int_{(l-1/2)F_s}^{(l+1/2)F_s} X_a(F) e^{j2\pi \frac{F}{F_s} n} dF = \sum_{l=-\infty}^{\infty} \int_{-F_s/2}^{F_s/2} X_a(F + lF_s) e^{j2\pi \frac{F+lF_s}{F_s} n} dF \tag{7.9}$$

Swapping the integral and the summation sign on the right hand side of (7.9), and noting that:

$$e^{j2\pi \frac{F+lF_s}{F_s} n} = e^{j2\pi \frac{lF_s}{F_s} n} e^{j2\pi \frac{F}{F_s} n} = e^{j2\pi \frac{F}{F_s} n} \tag{7.10}$$

we obtain:

$$\sum_{l=-\infty}^{\infty} \int_{-F_s/2}^{F_s/2} X_a(F + lF_s) e^{j2\pi \frac{F+lF_s}{F_s} n} dF = \int_{-F_s/2}^{F_s/2} \sum_{l=-\infty}^{\infty} X_a(F + lF_s) e^{j2\pi \frac{F_s}{F_s} n} dF \tag{7.11}$$

Comparing (7.7) and (7.11) we obtain:

$$\frac{1}{F_s}\int_{-F_s/2}^{F_s/2} X\left(\frac{F}{F_s}\right)e^{j2\pi\frac{F}{F_s}n}\,dF = \int_{-F_s/2}^{F_s/2}\sum_{l=-\infty}^{\infty} X_a(F+lF_s)e^{j2\pi\frac{F_s}{F_s}n}\,dF \tag{7.12}$$

And hence, from (7.12), one can deduce the relation:

$$X\left(\frac{F}{F_s}\right) = F_s\sum_{l=-\infty}^{\infty} X_a(F+lF_s) \text{ or}$$

$$X(f) = F_s\sum_{l=-\infty}^{\infty} X_a\left[(f+l)\right]F_s \tag{7.13}$$

The relation in (7.13) implies that the spectrum of $X(f)$ is made up of replicas of the analog spectrum $X_a(F)$ periodically shifted in frequency and scaled by the sampling frequency F_s as shown in Figure 7.1.

The relationship in (7.13) expresses the association between the analog spectrum and its discrete counterpart. The discrete spectrum is essentially made up of a series of periodic replicas of the analog spectrum. If the sampling frequency F_s is selected such that $F_s \geq B$, where B is the IF bandwidth not to be confused with the baseband bandwidth, which is only the positive half of the spectrum, the analog signal can then be reconstructed without loss of information due to aliasing from the discrete signal via filtering scaled by F_s. Note that the minimum sampling frequency allowed to reconstruct the analog signal from its discrete-time counterpart is $F_s = B$. This frequency is known as the Nyquist rate. However, if F_s is chosen such that $F_s < B$, then the reconstructed analog signal suffers from loss of information due to aliasing, as shown in Figure 7.1(c) and (d), and an exact replica of the original analog signal cannot be faithfully reproduced. In this case, as can be seen from Figure 7.1(c), the discrete spectrum is made up of scaled overlapped replicas of the original spectrum $X_a(F)$. The reconstructed signal is corrupted with aliased spectral components coexisting on top of the original spectral components as can be seen in Figure 7.1(d), thus preventing us from recreating the original analog signal.

7.1.2 Out-of-Band Energy

A band-limited lowpass signal is theoretically defined as a signal that has no frequency components above a certain upper frequency. Similarly, a bandpass band-limited signal is a

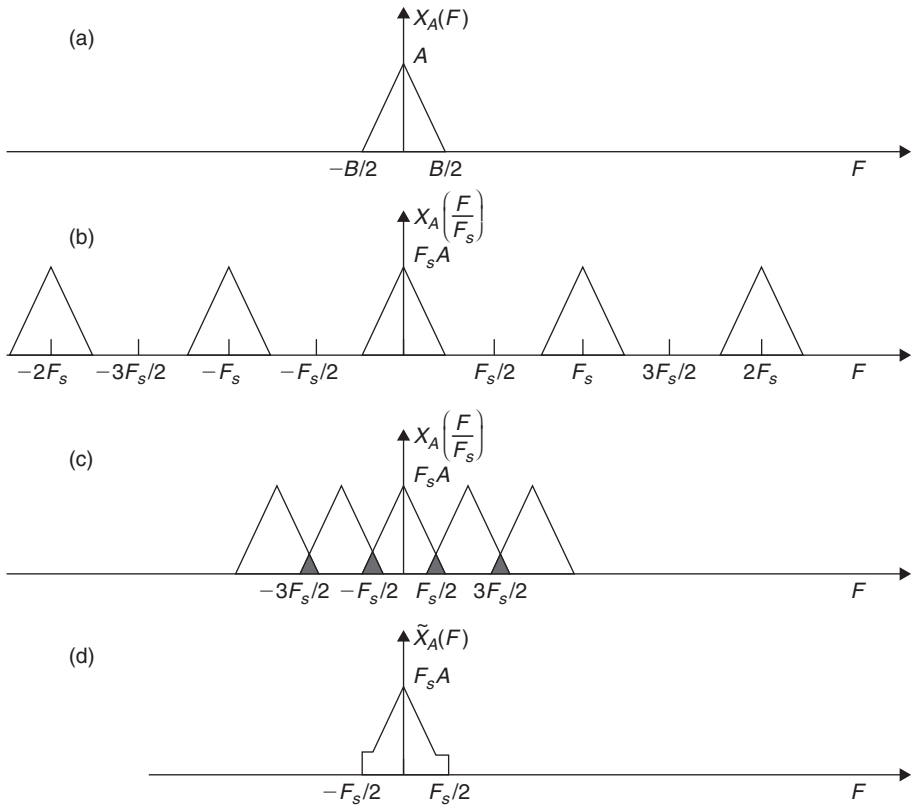

Figure 7.1 Lowpass sampling of analog signals: (a) spectrum of analog bandlimited signal, (b) spectrum of discrete-time sampled analog signal scaled by F_s and replicated, (c) aliased spectrum of discrete-time sampled signal, and (d) spectrum of reconstructed analog signal derived from aliased discrete-time signal in (c)

signal that is bounded by a certain lower frequency limit and a certain upper frequency limit. In reality, however, a received signal at an antenna is not strictly band-limited per the definition just given. Certain out-of-band frequency components are attenuated via filtering but not entirely eliminated. Thermal noise, which is white Gaussian in nature, is also always present at the input of the ADC. This out-of-band energy at the input of the ADC must be managed properly in order to minimize the distortion imposed on the desired signal by aliasing. Therefore, one key question the designer must ask is: how much SNR degradation is tolerable?

In order to answer the question properly, the analysis must take into account the entire receive-chain, and consider the sampling frequency and the location of the aliased signal components. What is meant by the latter is whether the aliased distortion components lie within the signal bandwidth or not. In the event where the aliased distortion does not overlap the desired signal after sampling, digital filtering can be used to recover the desired signal; otherwise the designer must solely rely on the performance of the antialiasing filter. The anti-aliasing filter must be designed such that performance distortion due to spectral overlap is less than the largest ADC spur appearing between DC and the Nyquist rate, as well as less than ½ LSB. These requirements tend to be very stringent on the filter design and can be alleviated by oversampling the signal and spreading the spectral replicas farther apart. Oversampling enables less complex anti-aliasing filter design with gradual roll-off at the expense of higher complexity and power consumption at the ADC. Oversampling requires that the ADC run at a faster clock rate, thus increasing the power consumption and complexity of the circuitry.

7.1.3 Reconstruction of Lowpass Signals

The Fourier transform of the analog signal $x_a(t)$ is:

$$x_a(t) = \int_{-\infty}^{\infty} X_a(F) e^{j2\pi Ft} dF \tag{7.14}$$

Assume for simplicity's sake that the discrete-time signal is sampled at the Nyquist rate $F_s = B$, that is:

$$X_a(F) = \begin{cases} \frac{1}{F_s} X\left(\frac{F}{F_s}\right) & -\frac{F_s}{2} < F < \frac{F_s}{2} \\ 0 & \text{otherwise} \end{cases} \tag{7.15}$$

Substituting the relation in (7.15) into (7.14), we obtain:

$$\hat{x}_a(t) = \frac{1}{F_s} \int_{-F_s/2}^{F_s/2} X\left(\frac{F}{F_s}\right) e^{j2\pi Ft} dF \tag{7.16}$$

where $\hat{x}_a(t)$ is the reconstructed analog signal. Recall that the Fourier transform of $X\left(\frac{F}{F_s}\right)$ is given as:

$$X\left(\frac{F}{F_s}\right) = \sum_{n=-\infty}^{\infty} x(nT_s) e^{-j2\pi \frac{F}{F_s} n} \tag{7.17}$$

where T_s is the sampling rate. Substituting (7.17) into (7.16), it becomes:

$$\hat{x}_a(t) = \frac{1}{F_s}\int_{-F_s/2}^{F_s/2}\left\{\sum_{n=-\infty}^{\infty} x(nT_s)e^{-j2\pi\frac{F}{F_s}n}\right\}e^{j2\pi Ft}dF \tag{7.18}$$

Rearranging the order of the summation and integral in (7.18):

$$\hat{x}_a(t) = \sum_{n=-\infty}^{\infty} x(nT_s)\left\{\frac{1}{F_s}\int_{-F_s/2}^{F_s/2} e^{j2\pi F\left(t-\frac{n}{F_s}\right)}dF\right\} \tag{7.19}$$

The integral in (7.19) is the sinc function:

$$\frac{1}{F_s}\int_{-F_s/2}^{F_s/2} e^{j2\pi F\left(t-\frac{n}{F_s}\right)}dF = \frac{1}{F_s}\frac{e^{j2\pi\frac{F_s}{2}\left(t-\frac{n}{F_s}\right)} - e^{-j2\pi\frac{F_s}{2}\left(t-\frac{n}{F_s}\right)}}{j2\pi\left(t-\frac{n}{F_s}\right)} = \frac{1}{F_s}\frac{\sin\left(2\pi\frac{F_s}{2}\left(t-\frac{n}{F_s}\right)\right)}{\pi\left(t-\frac{n}{F_s}\right)}$$

$$\frac{1}{F_s}\int_{-F_s/2}^{F_s/2} e^{j2\pi F\left(t-\frac{n}{F_s}\right)}dF\Bigg|_{T_s=\frac{1}{F_s}} = \frac{\sin\left(\frac{\pi}{T_s}(t-nT_s)\right)}{\frac{\pi}{T_s}(t-nT_s)} \tag{7.20}$$

Hence, substituting (7.20) into (7.19), it becomes:

$$\hat{x}_a(t) = \sum_{n=-\infty}^{\infty} x(nT_s)\frac{\sin\left(\frac{\pi}{T_s}(t-nT_s)\right)}{\frac{\pi}{T_s}(t-nT_s)} \tag{7.21}$$

The reconstructed analog signal in (7.21) involves weighing each individual discrete sample by a *sinc* function shifted-in-time by the sampling period. The *sinc* function:

$$p(t) = \frac{\sin\left(\frac{\pi}{T_s}(t-nT_s)\right)}{\frac{\pi}{T_s}(t-nT_s)} \tag{7.22}$$

is known as the ideal interpolation filter expressed in the frequency domain as:

$$P(F) = \begin{cases} 1 & |F| < F_s/2 \\ 0 & |F| \geq F_s/2 \end{cases} \tag{7.23}$$

Applying the ideal interpolation filter in (7.23) to the spectrum of a nonaliased discrete-time signal results in recovering the original analog signal without any loss of information, as shown in Figure 7.2.

Therefore, another simple way to arrive at the relationship expressed in (7.21) is to start with filtering the spectrum of the discrete-time signal by the interpolation filter (7.23), that is:

$$\hat{X}\left(\frac{F}{F_s}\right) = X\left(\frac{F}{F_s}\right) P(F) \tag{7.24}$$

Multiplication in the frequency domain is convolution in the time domain,

$$\hat{x}_a(t) = x_a(t) * p(t) = \sum_{n=-\infty}^{\infty} x(nT_s) \frac{\sin\left(\frac{\pi}{T_s}(t - nT_s)\right)}{\frac{\pi}{T_s}(t - nT_s)} \tag{7.25}$$

which is none other than the relationship developed in (7.21). Note that certain modulation schemes require a flat response at the output of the DAC. Hence, the inband distortion due to the weighing function of the *sinc* must be corrected for. This is typically done with an equalizer mimicking an inverse *sinc* filter.

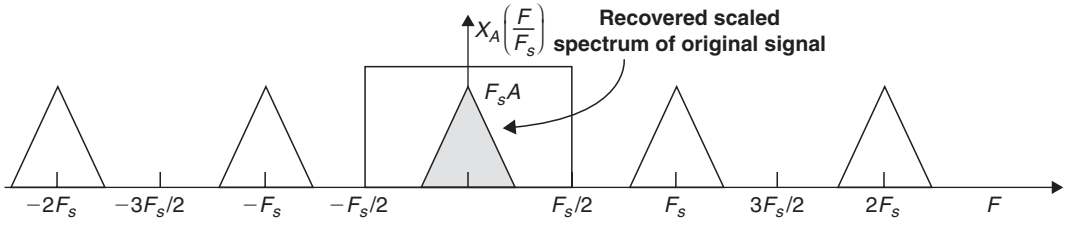

Figure 7.2 Recovered sampled spectrum of original analog signal

7.2 Sampling of Bandpass Signals

The sampling process is critical for radio receivers that digitize signals at RF or IF. Sampling an analog signal at IF or RF results in replicas of the signal's spectrum repeated at uniform intervals. The choice of the sampling rate of such signals is dependent on the signal's bandwidth and the IF or RF center frequency.

Bandpass sampling does not require the use of analog quadrature mixing, thus eliminating certain DC offsets due to the carrier feedthrough in the mixers, VGA gain stages, and filters. Furthermore, it does not require analog phase and amplitude compensation due to IQ imbalance. Bandpass sampling requires only one ADC, as shown in Figure 7.3, allowing for the final IF (or low IF) to baseband conversion to occur in the digital domain. Note that the second DAC feeding off the phase-to-accumulator block is not a transmit DAC, but rather generates a sinusoid as part of the direct digital synthesis (DDS) block. A DDS system is a mechanism for generating a sinusoid digitally and passing the signal through a DAC to be used for mixing.

On the other hand, bandpass sampling is sensitive to carrier or IF frequency variations, as well as sampling frequency and jitter. In this case, the ADC tends to consume more power due to a faster sample and hold (S/H) and digital circuitry and the performance of the system becomes more prone to degradations due to mixed-signal circuit imperfections. Furthermore, the requirements imposed on the bandpass filter at IF before the ADC become much more stringent and much more difficult to build compared to the more benign lowpass filters used in analog quadrature downconversion. Note that this IF filter also performs the function of an antialiasing filter used in the lowpass case.

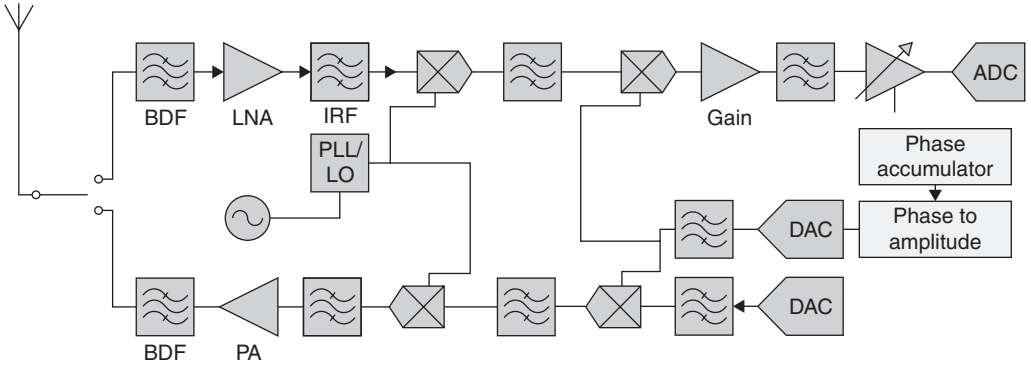

Figure 7.3 IF sampling architecture showing the use of only one ADC and one DAC

7.2.1 Representation of Bandpass Signals

Consider the conceptual modulator depicted in Figure 7.4. The in-phase $I(t)$ and quadrature $Q(t)$ signals are obtained from discrete-time signals converted to analog by two DACs. The signal at IF, or RF in the case of a direct conversion transmitter, can be expressed as:

$$x_a(t) = I(t)\cos(2\pi F_c t) - Q(t)\sin(2\pi F_c t) \tag{7.26}$$

again, where $I(t)$ and $Q(t)$ are the real and complex components of the complex analog baseband signal $s_a(t) = I(t) - jQ(t)$. The bandpass signal can then be related to the complex baseband signal as:

$$x_a(t) = \mathrm{Re}\left\{s_a(t)e^{j2\pi F_c t}\right\} = \mathrm{Re}\left\{(I(t) + jQ(t))e^{j2\pi F_c t}\right\} \tag{7.27}$$

Furthermore, the relation in (7.26) can be expressed as:

$$x_a(t) = \sqrt{I^2(t) + Q^2(t)}\cos\left(2\pi F_c t + \tan^{-1}\left(\frac{-Q(t)}{I(t)}\right)\right) \tag{7.28}$$

7.2.2 Sampling of Bandpass Signals — Integer Positioning

The fractional bandwidth is typically referred to as the fractional number of bandwidths separating the origin to the lower edge of the passband [1]. Integer band positioning is a

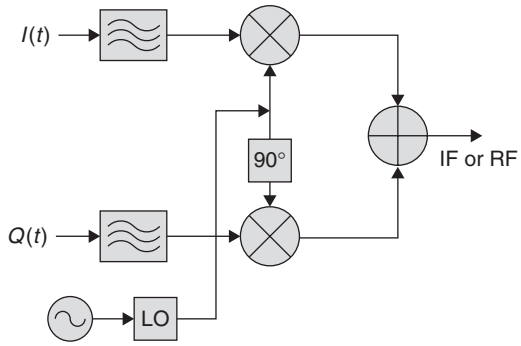

Figure 7.4 Conceptual upconversion of baseband signal to IF or RF frequency

special case where the lower or upper edge of the band is located at an integer multiple of bandwidths from the origin, that is:

$$F_c \pm \frac{B}{2} = lB \qquad l \text{ is a positive integer} \tag{7.29}$$

An example for integer band positioning for $l = 5$ for $F_c + \frac{B}{2} = 5B$ is depicted in Figure 7.5.

Note that one important consideration concerning the bandwidth of the sampled signal implies that the signal is bounded by a lower frequency component F_l and an upper frequency component F_u such that B is equal to the interval (F_l, F_u) such that there are no signal components at either F_l or F_u. This assumption will hold true throughout this discussion and will be elaborated upon when discussing the general bandpass sampling case.

Assume that the carrier frequency (or IF frequency before the ADC) is chosen such that:

$$F_c + \frac{B}{2} = lB \qquad l \text{ is a positive integer} \tag{7.30}$$

Sampling (7.26) at the rate $T_s = 1/2B$ and substitute $F_c = (2l - 1)\frac{B}{2}$, we obtain:

$$\begin{aligned} x_a(nT_s) &= I(nT_s)\cos\left(2\pi(2l-1)\frac{B}{2}nT_s\right) - Q(nT_s)\sin\left(2\pi(2l-1)\frac{B}{2}nT_s\right) \\ x_a(nT_s) &= I(nT_s)\cos\left(\frac{\pi}{2}(2l-1)n\right) - Q(nT_s)\sin\left(\frac{\pi}{2}(2l-1)n\right) \end{aligned} \tag{7.31}$$

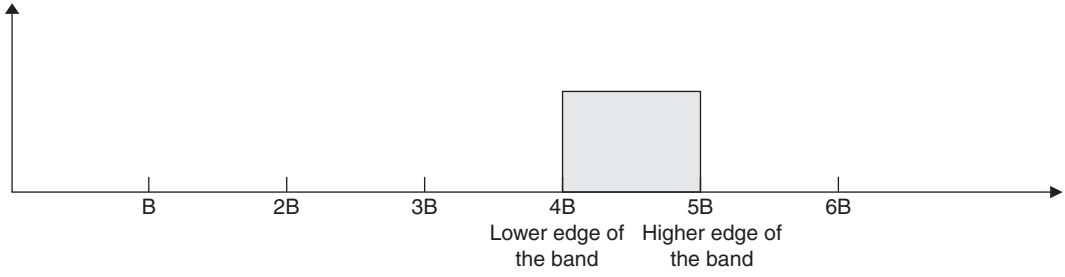

Figure 7.5 Example of integer band positioning for $l = 4$

Let's consider the two cases where n is even and n is odd. For n even, that is $n = 2m$, the relation in (7.31) becomes:

$$\begin{aligned} x_a(2mT_s) &= I(2mT_s)\cos((2l-1)m\pi) - Q(nT_s)\sin((2l-1)m\pi) \\ x_a(2mT_s) &= (-1)^m I(2mT_s) \text{ or } x_a(nT_s) = (-1)^{n/2} I(nT_s) \text{ for } n \text{ even} \end{aligned} \tag{7.32}$$

For n odd, that is $n = 2m - 1$, the relation in (7.31) becomes:

$$\begin{aligned} x_a((2m-1)T_s) &= I((2m-1)T_s)\cos\left(2\pi(2l-1)\frac{B}{2}(2m-1)T_s\right) \\ &\quad - Q((2m-1)T_s)\sin\left(2\pi(2l-1)\frac{B}{2}(2m-1)T_s\right) \\ x_a((2m-1)T_s) &= I((2m-1)T_s)\cos\left(\frac{\pi}{2}(4lm-2l-2m+1)\right) \\ &\quad - Q((2m-1)T_s)\sin\left(\frac{\pi}{2}(4lm-2l-2m+1)\right) \\ x_a((2m-1)T_s) &= (-1)^{l+m+1}Q((2m-1)T_s) \text{ or } x_a(nT_s) = (-1)^{l+\frac{n+1}{2}+1}Q(nT_s) \text{ for } n \text{ odd} \end{aligned} \tag{7.33}$$

Let $T_s' = 2T_s = 1/B$ and using the relations expressed in (7.32) and (7.33) we can represent the sampled signal in yet another form:

$$\begin{aligned} x_a(mT_s') &= (-1)^m I(mT_s') && \text{for } n \text{ even} \\ x_a\left(mT_s' - \frac{T_s'}{2}\right) &= (-1)^{l+m+1}Q\left(mT_s' - \frac{T_s'}{2}\right) && \text{for } n \text{ odd} \end{aligned} \tag{7.34}$$

Observation

With this choice of relationship between the sampling rate and the bandwidth of the IF signal, we note that the even-numbered samples are related to the in-phase baseband signal $I(t)$ whereas the odd-numbered samples are related to the quadrature baseband signal $Q(t)$. Therefore, at the output of the ADC sampling at IF, the quadrature conversion to baseband is rather simple. To obtain the in-phase digital component of the sampled signal, it is sufficient to digitally multiply the signal at the output of the ADC by $(-1)^{n/2}$ for even n and by 0 for odd n. Similarly, in order to obtain the digital quadrature component of the received signal, it is sufficient to digitally multiply the output of the ADC by $(-1)^{l+\frac{n+1}{2}+1}$ for n odd and by 0 for n even.

7.2.3 Reconstruction of Bandpass Signal — Integer Positioning

The discrete samples of the in-phase and quadrature components of (7.34), that is $I(mT_s^{'})$ and $Q\left(mT_s^{'} - \frac{T_s^{'}}{2}\right)$, can be used to reconstruct the equivalent analog lowpass signals according to the relationship developed in (7.21) as:

$$I(t) = \sum_{m=-\infty}^{\infty} I(2mT_s) \frac{\sin\left(\frac{\pi}{2T_s}(t - 2mT_s)\right)}{\frac{\pi}{2T_s}(t - 2mT_s)}$$

$$Q(t) = \sum_{m=-\infty}^{\infty} Q(2mT_s - T_s) \frac{\sin\left(\frac{\pi}{2T_s}(t - 2mT_s + T_s)\right)}{\frac{\pi}{2T_s}(t - 2mT_s + T_s)} \tag{7.35}$$

Substituting (7.34) and (7.35) into (7.26), we can express the analog bandpass signal as:

$$x_a(t) = I(t)\cos(2\pi F_c t) - Q(t)\sin(2\pi F_c t)$$

$$x_a(t) = \sum_{m=-\infty}^{\infty} \left\{ (-1)^m x_a(2mT_s) \frac{\sin\left(\frac{\pi}{2T_s}(t - 2mT_s)\right)}{\frac{\pi}{2T_s}(t - 2mT_s)} + \right.$$

$$\left. (-1)^{l+m} x_a(2mT_s - T_s) \frac{\sin\left(\frac{\pi}{2T_s}(t - 2mT_s + T_s)\right)}{\frac{\pi}{2T_s}(t - 2mT_s + T_s)} \right\} \tag{7.36}$$

The relationship in (7.36) can be further expressed as:

$$x_a(t) = \sum_{m=-\infty}^{\infty} x_a(mT_s) \frac{\sin\left(\frac{\pi}{2T_s}(t - mT_s)\right)}{\frac{\pi}{2T_s}(t - mT_s)} \cos\left(2\pi F_c(t - mT_s)\right) \tag{7.37}$$

where again the sampling rate is twice the IF bandwidth B, that is $T_s' = 1/2B$.

7.2.4 Sampling of Bandpass Signals — Half-Integer Positioning

Half-integer positioning refers to the special case for which the bandwidth of the desired signal is centered at an integer multiple of the bandwidth, that is:

$$F_c = lB \qquad l \text{ is a positive integer} \tag{7.38}$$

Figure 7.6 shows an example of half-integer band positioning for $l = 4$.

For this case, we present a special case of interest which results in a simplified digital quadrature demodulator. Assume that the sampling rate $F_s = 4B$. Sampling (7.26) at the rate $T_s = 1/4B$ and substituting $F_c = lB$, we obtain:

$$\begin{aligned} x_a(nT_s) &= I(nT_s)\cos(2\pi lBnT_s) - Q(nT_s)\sin(2\pi lBnT_s) \\ x_a(nT_s) &= I(nT_s)\cos\left(\frac{\pi l}{2}n\right) - Q(nT_s)\sin\left(\frac{\pi l}{2}n\right) \end{aligned} \tag{7.39}$$

Note for the case where l is even, the product ln is always even whether n is odd or even. For this scenario, let $l = 2k$, then the cosine and sine argument in (7.39) is πkn and hence (7.39) reduces to:

$$x_a(nT_s) = (-1)^{kn} I(nT_s) \tag{7.40}$$

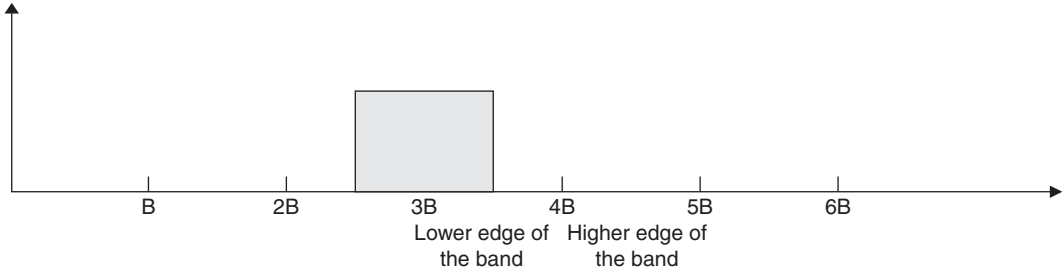

Figure 7.6 Example of half-integer band positioning for $l = 4$

This is true since $\sin(\pi kn) = 0$ for all values of k and n, and therefore the information on the quadrature component $Q(.)$ could never be recovered. Hence, we conclude that l even is not a viable choice for this sampling rate. Next, we consider the case where l is odd. In this case, the relationship in (7.39) can be expressed as:

$$x_a(nT_s) = I(nT_s)\cos(\pi) - Q(nT_s)\sin(2\pi lBnT_s)$$
$$x_a(nT_s) = \begin{cases} (-1)^{n/2} I(nT_s) & n \text{ is even} \\ (-1)^{\frac{l+n}{2}} Q(nT_s) & n \text{ is odd} \end{cases} \tag{7.41}$$

The reconstruction of bandpass signal due to half-integer positioning is developed in a very similar fashion to that of the integer positioning case.

7.2.5 Nyquist Zones

Nyquist zones subdivide the spectrum into regions spaced uniformly at intervals of $F_s/2$. Each Nyquist zone contains a copy of the spectrum of the desired signal or a mirror image of it. The odd Nyquist zones contain exact replicas of the signal's spectrum—that is, if the original signal is centered at F_c ($F_c = 0$ is the lowpass signal case)—the exact spectral replica will appear at $F_c + kF_s$ for $k = 0, 1, 2, 3 \ldots$. The zone corresponding to $k = 0$ is known as the first Nyquist zone, whereas the third and fifth Nyquist zones correspond to $k = 1$ and $k = 2$, respectively.

Similarly, mirrored replicas of the signal's spectrum occur in even numbered Nyquist zones, that is the spectra are centered at $kF_s - F_c$ for $k = 1, 2, 3 \ldots$. The second Nyquist zone corresponds to $k = 1$ whereas the fourth and sixth Nyquist zones correspond to $k = 2$ and $k = 3$, respectively. An example depicting odd and even Nyquist zones is given in Figure 7.7.

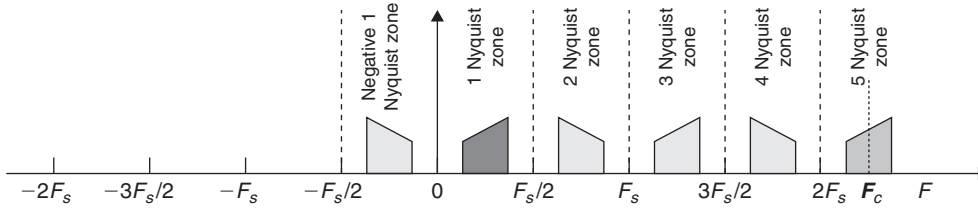

Figure 7.7 Spectral images of desired signal depicted in various Nyquist zones

A relationship between the signal's center frequency F_c at RF or IF can be expressed as:

$$F = \begin{cases} rem(F_c, F_s) & \left\lfloor \frac{F_c}{F_s/2} \right\rfloor \text{ is even implying that image is exact replica} \\ F_s - rem(F_c, F_s) & \left\lfloor \frac{F_c}{F_s/2} \right\rfloor \text{ is odd implying that image is mirrored replica} \end{cases} \quad (7.42)$$

where *rem* is the remainder after division, $\lfloor \cdot \rfloor$ denotes the floor function, which rounds a number towards zero, and F is the center frequency of the image in the first Nyquist zone.

7.2.6 Sampling of Bandpass Signals — General Case

Bandpass sampling can be utilized to downconvert a signal from RF or IF to a bandpass signal at a lower IF. The bandpass signal is repeated at integer multiples of the sampling frequency. Therefore choosing the proper spectral replica of the original bandpass signal allows for downconversion. Ideally, as mentioned earlier, a bandpass signal has no frequency components below a certain frequency F_L or above a certain frequency F_U, that is, the signal or channel bandwidth is strictly defined by the bandwidth $B = F_U - F_L$.

Let the center frequency of the signal or channel F_c be defined as $F_c = F_U - B/2 = F_L + B/2$, then the bandpass sampling frequency for normal or exact spectral placement is given as [1]–[3]:

$$\frac{2F_c + B}{2n+1} \le F_s \le \frac{F_c - B/2}{n} \quad 0 \le n \le \left\lfloor \frac{F_c - B/2}{2B} \right\rfloor \text{ normal spectral placement} \quad (7.43)$$

In a similar vein, for the inverted or mirrored-replica spectral placement of the signal, the sampling frequency is given as:

$$\frac{F_c + B/2}{n} \le F_s \le \frac{2F_c - B}{2n-1} \quad 1 \le n \le \left\lfloor \frac{F_c + B/2}{2B} \right\rfloor \text{ inverted spectral placement} \quad (7.44)$$

The minimum sampling rates expressed in (7.43) and (7.44) do not take into account any instabilities or imperfections of the carrier or sampling frequencies [1],[4], and [5]. Therefore, when choosing a sampling frequency, the designer must take into account these imperfections to avoid any serious SNR degradation due to aliasing of the signal.

Example 7-1: Sampling of Fixed WiMAX Signals

The relationship between the sampling factor and the channel bandwidth for fixed WiMAX is shown in Table 7.1. Given this relationship, the signal versus channel bandwidth for the various signaling schemes is expressed in Table 7.2. Choose an IF center frequency of 200 MHz. Based on the boundaries defined in (7.43) and (7.44), compute the sampling rate boundaries for maximum n.

The analyses for this example are summarized in Table 7.3 and Table 7.4. It would be instructive for the reader to repeat the example for an IF frequency of 175 MHz and note what happens to the sampling rate in each case and why.

Table 7.1 Sampling factor versus nominal signal bandwidth for fixed WiMAX

Sampling Factor	Nominal Channel Bandwidth
8/7	Signal BWs that are multiples of 1.75 MHz
28/25	Signal BW that are multiples of 1.25, 1.5, 2, or 2.75
8/7	For all others not specified

Table 7.2 Signal versus channel bandwidth for fixed WiMAX

Signal Bandwidth (MHz)	Channel Bandwidth (MHz)
20	22.4
10	11.2
8.75	10
7	8
5	5.6

Table 7.3 Sampling rate boundaries for the 22.4 and 11.2 MHz channel BW case

Parameter	Value	Value
Bandwidth (MHz)	22.40	11.20
IF frequency (MHz)	200.00	200.00
f_h (MHz)	211.20	205.60
f_l (MHz)	188.80	194.40
maximum n	4.00	8.00
High sampling boundaries based on *n* max (MHz)	47.20	24.30
Low sampling boundaries based on *n* max (MHz)	46.93	24.19

Table 7.4 Sampling rate boundaries for the 10, 8, and 5.6 MHz channel BW case

Parameter	Value	Value	Value
Bandwidth (MHz)	10.00	8.00	5.60
IF frequency (MHz)	200.00	200.00	200.00
f_h (MHz)	205.00	204.00	202.80
f_l (MHz)	195.00	196.00	197.20
maximum *n*	9.00	12.00	17.00
High sampling boundaries based on *n* max (MHz)	21.67	16.33	11.60
Low sampling boundaries based on *n* max (MHz)	21.58	16.32	11.59

7.3 The AGC Algorithm

The purpose of the automatic gain control (AGC) algorithm is to regulate the received signal strength at the input of the ADCs such that the required signal SNR for proper decoding is met. For example, if the received signal strength is weak at the antenna, the AGC algorithm boosts the receiver gain stages in order to minimize the noise and bring the signal level to an acceptable SNR. Likewise, if the received signal strength is strong, the AGC algorithm attenuates the receiver gain stages in order to avoid signal clipping and nonlinear degradations that would otherwise deteriorate the signal SNR. In receivers that employ modern digital modulation techniques, the AGC corrects for long term fading effects due to shadowing. The short term fast fades, especially those denoted as frequency selective fades, are corrected for in the digital equalizer, be it a RAKE receiver, a decision feedback equalizer (DFE), or any other form of equalization designed to deal with this type of fading. After equalization, any remaining symbols in error are corrected, or attempted to be corrected, in the forward error correction block using a variety of appropriate coding schemes. It is important to note that the AGC must not correct for fast fades especially within a data slot, or a block of symbols within frame. Performing amplitude gain control within a coherent block of data could serve to adversely affect the equalizer or forward error correction.

The AGC loop mostly controls various analog gain and attenuation blocks at various points in the receive chain. For example, in a superheterodyne receiver, depicted in

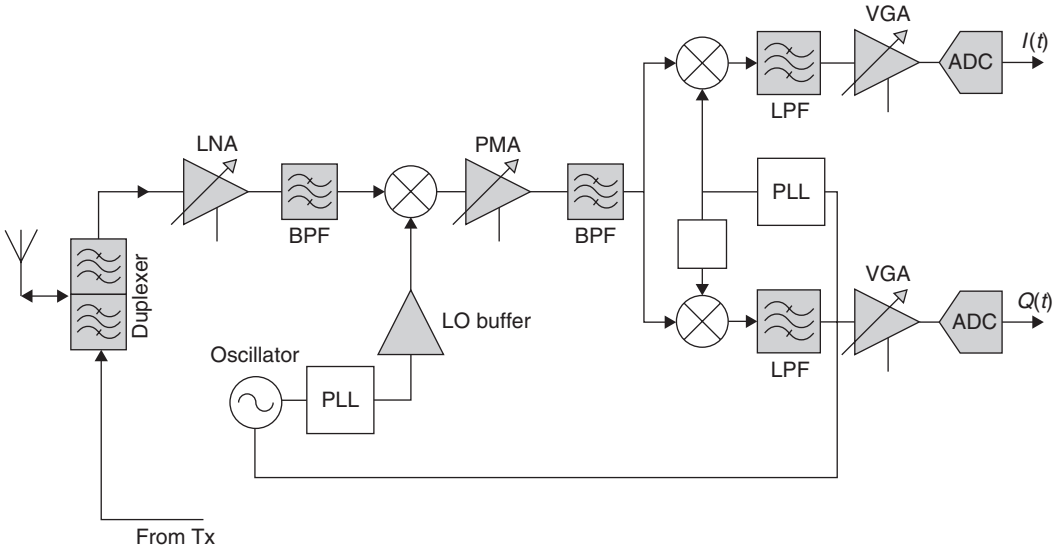

Figure 7.8 Block diagram of superheterodyne receiver

Figure 7.8, the AGC loop could switch the LNA gain from low-setting to high setting and vice versa, perform a similar function concerning the post mixer amplifier (PMA), and vary the gain of the voltage gain amplifier (VGA) to maintain a certain signal level relative to the noise in the receiver thus maintaining an acceptable SNR. The object of this discussion is not how to control the receiver line-up, but rather how to design the digital loop that estimates the input signal power and adjusts the gain accordingly to maintain a satisfactory SNR. The following analysis is applicable to most common receiver line-up architectures.

7.3.1 The Loop Detector

The first order AGC loop is depicted in Figure 7.9. The analog in-phase and quadrature input signals $I(t)$ and $Q(t)$ undergo amplifications or attenuation by the in-phase and quadrature VGAs as well as the LNA and PMA gain stages. At the output of the ADCs the discrete in-phase and quadrature signals are then squared and added to generate the instantaneous signal power:

$$r^2(n) = I^2(n) + Q^2(n) = I^2(t) + Q^2(t)\Big|_{t=nT_s} \tag{7.45}$$

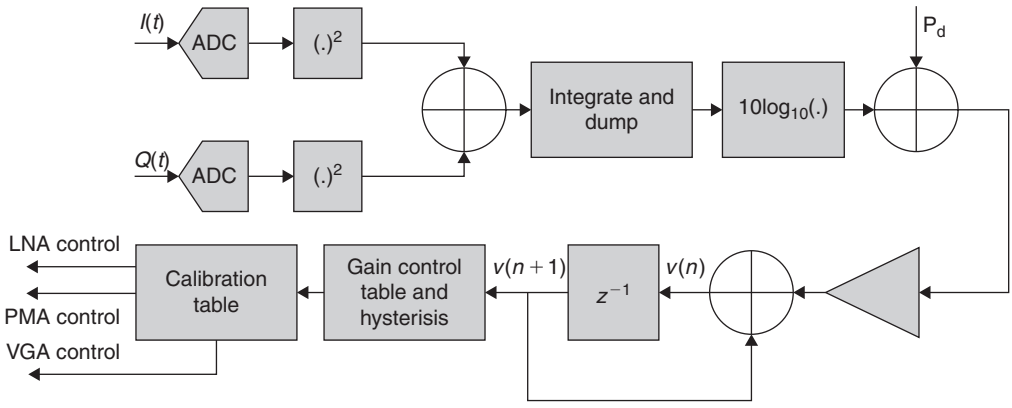

Figure 7.9 The AGC loop

The instantaneous output power provided in (7.43) is obtained at the output of the detector. Most practical detectors, however, implement an approximation to (7.45) or its square root in order to simplify the digital ASIC implementation. The most common approximation takes the form:

$$r(n) \approx \alpha \max\left\{I(n), Q(n)\right\} + \beta \min\left\{I(n), Q(n)\right\} \tag{7.46}$$

The most commonly used approximation of the envelope based on (7.46) is:

$$r(n) \approx \frac{15}{16}\left[\max\left\{I(n), Q(n)\right\} + \frac{1}{2}\min\left\{I(n), Q(n)\right\}\right] \tag{7.47}$$

Other approximation examples include:

$$r(n) \approx \max\left\{I(n), Q(n)\right\} + \frac{1}{4}\min\left\{I(n), Q(n)\right\} \tag{7.48}$$

and:

$$r(n) \approx \max\left\{I(n), Q(n)\right\} + \frac{3}{8}\min\left\{I(n), Q(n)\right\} \tag{7.49}$$

In order to evaluate the performance of the various detectors of the form presented in (7.46), it is instructive to compare their performance with the exact detector presented in (7.45). To do so, let us compare the amplitude of (7.46) to the unity vector at the output of the exact

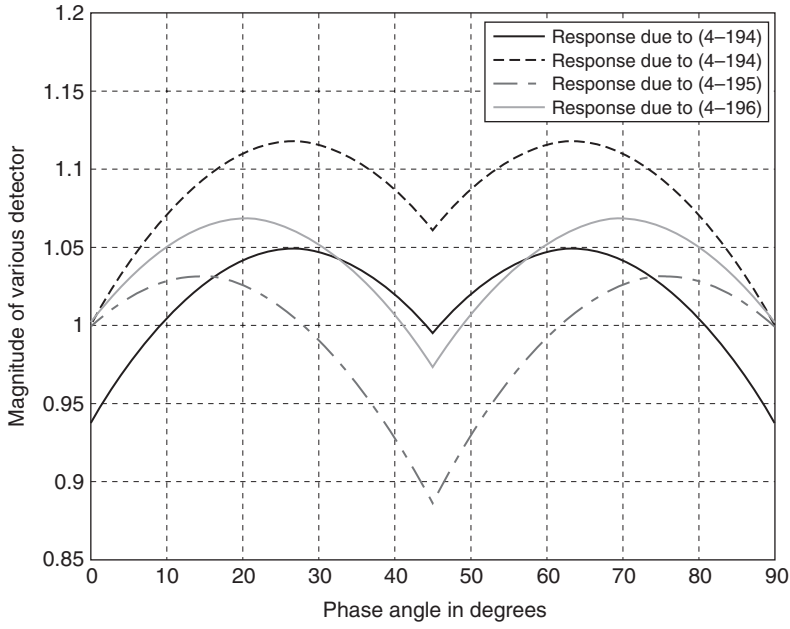

Figure 7.10 Performance of various AGC detectors based on (7.46)

detector, resulting from $I(n) = \cos(\theta)$ and $Q(n) = \sin(\theta)$. That is, compare the magnitude of (7.46) to 1 for various phase angles θ. The result of these comparisons is depicted in Figure 7.10. However, regardless of the detector used, its performance largely depends on the input data. For random white noise type input data, the performance of the AGC with an estimated detector approaches the performance of an AGC with an exact detector at the cost of reducing the attack and decay time resulting from reducing the gain value at the input of the loop filter.

In the ensuing analysis, only the true instantaneous power estimate based on (7.45) will be used. The output signals to the ADCs must not undergo any digital channel filtering before detecting the instantaneous output power in order to provide a true estimate of the signal power. This is essential, since a channel filter attenuates the interference or blocker and prevents the AGC from reacting properly to it. Certain AGC designs, however, rely on two instantaneous power estimates: one before the digital channel filters, which approximates the signal plus blocker power, and one estimate after the digital channel filters, which estimates the desired signal power without the effect of interference and blocking. In this discussion, we will limit our analysis to the case where the signal plus interference instantaneous power is used to perform gain control.

7.3.2 Loop Analysis

The integrate-and-dump function in Figure 7.9 serves to estimate the mean of the received signal power:

$$E\left\{r^2(n)\right\} = \frac{1}{N}\sum_{n=0}^{N-1}\left[I^2(n) + Q^2(n)\right] \tag{7.50}$$

Assume that the VGAs and gain stages can be modeled as linear functions of the form $10^{(.)/20}$; that is, the gain stages are operating in a linear fashion without compression and the VGA gains can be varied in a monotonically increasing or decreasing trend. Then the output of the loop filter after the delay element in Figure 7.9 can be represented in state space form:

$$\nu(n+1) = \nu(n) + \mu\left[P_d - 10\log_{10}\left(10^{\nu(n)/10}r^2(n)\right)\right] \tag{7.51}$$

where $\nu(n)$ is the state at the output of the loop filter, and the gain stage $10^{\nu(n)/20}$ is an approximation of the AGC's various gain stages operating in the linear region. P_d is the desired set power of the AGC. Its value is mainly dictated by the desired SNR of the received signal. In most cases, P_d is defined in terms of the back-off necessary from ADC full scale in order to ensure no clipping in the desired signal. In some cases, however, some clipping is allowed. This occurs when the signal PAR is large enough and statistically its peak occurs less than 5% of the time.

The expectation operator serves as a lowpass filter to remove the effect of zero-mean white noise. Further note that the gain is approximated as $10^{\nu(n)/20}$ and not as $10^{\nu(n)/10}$ since this is voltage gain and not power gain. The relation in (7.51) can be further expressed as

$$\begin{aligned}\nu(n+1) &= \nu(n) + \mu\left[P_d - \nu(n) - 10\log_{10}\left(\hat{r}^2(n)\right)\right] \\ &= (1-\mu)\nu(n) + \mu\left[P_d - 10\log_{10}\left(\hat{r}^2(n)\right)\right]\end{aligned} \tag{7.52}$$

where $\hat{r}^2(n) = E\left\{r^2(n)\right\}$ is the mean squared input power. The mean squared input power can be estimated via an integrate-and-dump function; that is:

$$\hat{r}^2(n) = E\left\{r^2(n)\right\} \approx \frac{1}{M}\sum_{m=0}^{M-1}\left\{I^2(n-m) + Q^2(n-m)\right\} \tag{7.53}$$

where the squared values of $I(n)$ and $Q(n)$ are summed over M-samples and then presented or *dumped* to the loop where the mean squared error value is then compared

with desired input signal level P_d. Note that the integrate and dump as a function is a lowpass filter; that is:

$$\begin{aligned} ID(z) &= 1 + z^{-1} + z^{-2} + \ldots + z^{-M+1} \\ &= \frac{1 - z^{-M}}{1 - z^{-1}} \end{aligned} \tag{7.54}$$

For a large M, the integrate-and-dump filter approximates the mean of the signal. By way of an example, compare the integrate-and-dump filter for $M = 30$ to the lowpass function $1/1 - z^{-1}$ which represents the true estimate of the mean. The results are depicted in Figure 7.11 and Figure 7.12. Note that in reality an exact mean estimator is not used if the AGC is not run in continuous mode. An integrate-and-dump version is used instead in order to *flush* the filter for various AGC updates. The length of the integration in terms of the number of samples M is typically programmable.

In the event where the in-phase and the quadrature signals resemble white Gaussian noise, the envelope $r^2(n)$ possesses a Rayleigh distribution. The distribution becomes Rician in the presence of a dominant narrowband signal.

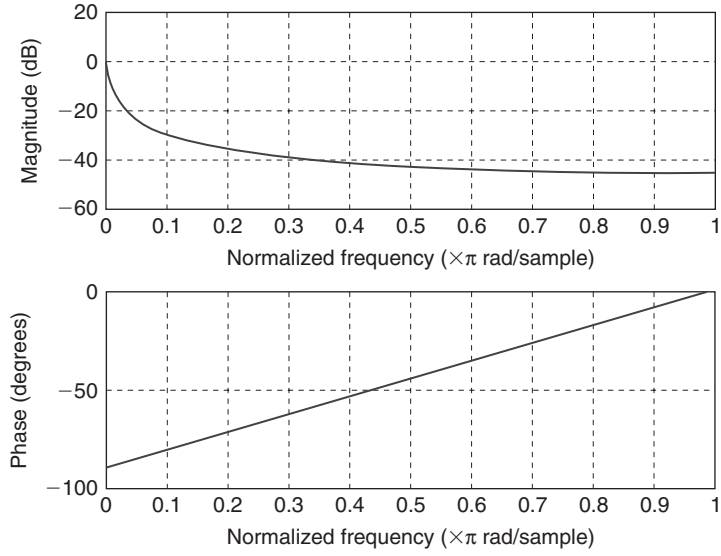

Figure 7.11 Filter response due to exact mean detector $1/1 - z^{-1}$

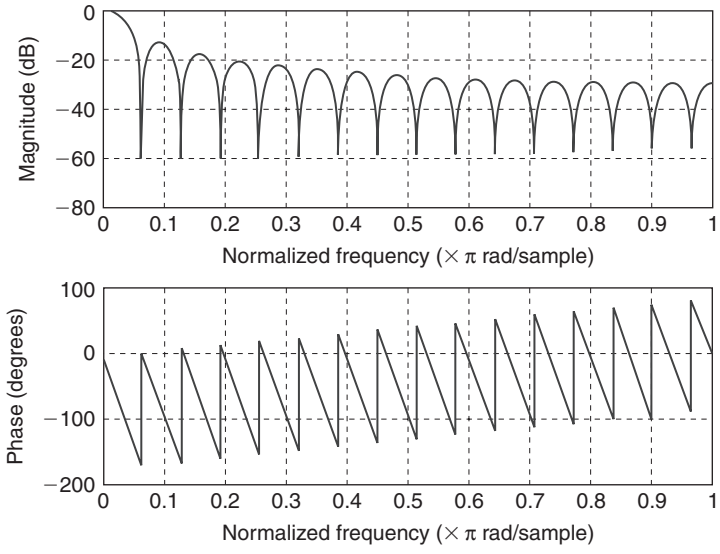

Figure 7.12 Filter response due to mean detector given in (7.54)

7.3.3 Steady State and Stability Analysis

During steady state, the mean of the error e_n is zero and $v(n+1) = v(n) = v$. The relation in (7.52) becomes:

$$\nu = (1-\mu)\nu + \mu\left[P_d - 10\log_{10}(\hat{r}^2(n))\right] \tag{7.55}$$

Solving for v in (7.55), we obtain the equilibrium point v as:

$$\nu = P_d - 10\log_{10}(\hat{r}^2(n)) \tag{7.56}$$

The equilibrium point in (7.56) is pivotal in computing the instantaneous dynamic range of the system.

Let $\chi(n)$ be the perturbation around the equilibrium point during steady state, then:

$$\nu + \chi(n+1) = (1-\mu)\left[\nu + \chi(n)\right] + \mu\left[P_d - 10\log_{10}(\hat{r}^2(n))\right] \tag{7.57}$$

Simplifying the relation in (7.57) we obtain:

$$\chi(n+1) = (1-\mu)\chi(n) - \mu\nu + \mu\left[P_d - 10\log_{10}(\hat{r}^2(n))\right] \tag{7.58}$$

Substituting (7.56) into (7.58) we obtain:

$$\begin{aligned}\chi(n+1) &= (1-\mu)\chi(n) - \mu\left[P_d - 10\log_{10}\left(\hat{r}^2(n)\right)\right] + \mu\left[P_d - 10\log_{10}\left(\hat{r}^2(n)\right)\right] \\ &= (1-\mu)\chi(n)\end{aligned} \tag{7.59}$$

The relation in (7.59) can be further expressed as:

$$\chi(n+1) = (1-\mu)^n\chi(0) \tag{7.60}$$

In order for the AGC loop to be stable, (7.60) must converge to zero as $n \to \infty$, thus imposing the relation:

$$\left|1-\mu\right| < 1 \Rightarrow \begin{cases}\mu > 0 \\ \mu < 2\end{cases} \tag{7.61}$$

In the above discussion, it is assumed that the AGC has the attack and decay times both dictated by the loop filter gain. Therefore, the linear AGC loop with a single pole loop filter is stable if and only if (7.61) is satisfied.

By way of an example, consider an input signal to the AGC consisting of a single sinusoid. The set of point of the AGC compared with the signal input power requires the AGC to adjust the input power by 65 dB. The output of the loop filter versus the number

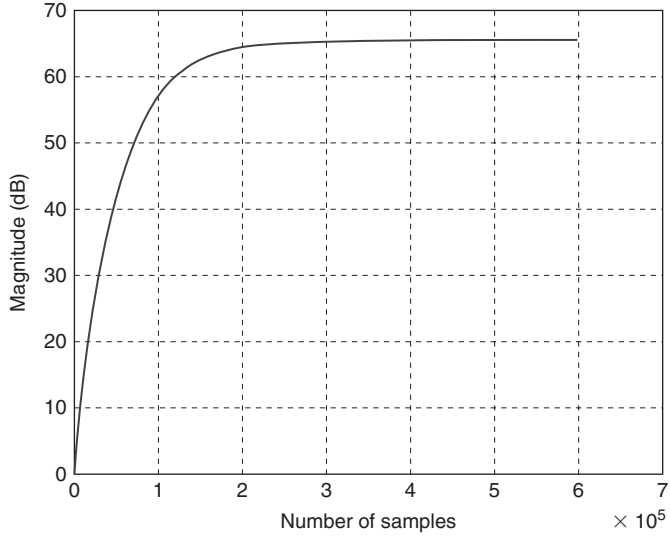

Figure 7.13 Output of loop filter feeding various gain stages as a function of time

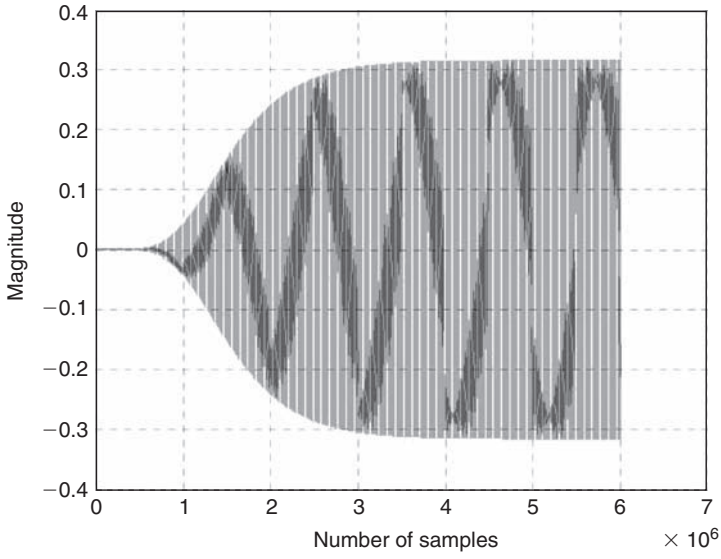

Figure 7.14 Input of in-phase signal to ADC as a function of time

of samples for a slowly but continuously adjusting AGC is shown in Figure 7.13. The in-phase input signal to the ADC as a function of the number of samples as its gain is being adjusted by the AGC is shown in Figure 7.14.

7.3.4 Peak to Average Power Ratio

7.3.4.1 PAR of a Single Tone Signal

Define the peak to average power ratio (PAR) of a given signal $r(t)$ as the ratio of the peak power of $r(t)$ to its average power:

$$PAR = 10\log_{10}\left(\frac{P_{peak}}{P_{avg}}\right) \tag{7.62}$$

For a single tone $r(t) = A\cos(2\pi F_c t)$, the PAR can be estimated as:

$$PAR = 10\log_{10}\left(\frac{P_{peak}}{P_{avg}}\right) = 10\log_{10}\left(\frac{\max\left\{\left|r(t)\right|^2\right\}}{F_c\int_0^{1/F_c} r^2(t)dt}\right) \tag{7.63}$$

The peak power of $r(t)$ can be simply found as:

$$P_{peak} = \max\left\{\left|A^2\cos^2(2\pi F_c t)\right|\right\} = A^2 \tag{7.64}$$

This is true obviously for the case where $t = 2n\pi$, $n = 0,1,\ldots$ On the other hand, the average power of $r(t)$ is found as:

$$\begin{aligned} P_{avg} &= F_c\int_0^{1/F_c} A^2\cos^2(2\pi F_c)dt \\ &= F_c\int_0^{1/F_c} A^2\left[\frac{1}{2}+\frac{1}{2}\cos(4\pi F_c t)\right]dt \\ &= \frac{F_c}{2}\left\{\frac{A^2}{F_c}+\underbrace{\int_0^{1/F_c} A^2\cos(4\pi F_c t)dt}_{=0}\right\} = \frac{A^2}{2} \end{aligned} \tag{7.65}$$

The PAR of $r(t)$ can then be estimated:

$$PAR = 10\log_{10}\left(\frac{P_{peak}}{P_s}\right) = 10\log_{10}\left(\frac{A^2}{A^2/2}\right) = 3dB \tag{7.66}$$

7.3.4.2 PAR of a Multi-Tone Signal

Next we extend the results obtained for a single tone in the previous section to a signal that possesses multiple tones. To simplify the analysis, consider the two-tone signal case first. Let the tones be harmonically related, that is $F_2 = MF_1$. This is certainly the case of OFDM signals where the various subcarriers are separated by a fixed frequency offset. Consider:

$$r(t) = A\cos(2\pi F_1 t) + B\cos(2\pi F_2 t) \tag{7.67}$$

The peak power of $r(t)$ can be found by first looking at the square of (7.67):

$$\begin{aligned} r^2(t) &= \left[A\cos(2\pi F_1 t) + B\cos(2\pi F_2 t)\right]^2 \\ &= \left[A^2\cos^2(2\pi F_1 t) + B^2\cos^2(2\pi F_2 t) + 2AB\cos(2\pi F_1 t)\cos(2\pi F_2 t)\right] \\ &= \frac{A^2}{2}+\frac{B^2}{2}+\frac{A^2}{2}\cos(4\pi F_1 t)+\frac{B^2}{2}\cos(4\pi F_2 t) \\ &\quad + AB\cos(2\pi(F_1-F_2)t) + AB\cos((F_1+F_2)t) \end{aligned} \tag{7.68}$$

The peak power of $r(t)$ can be found by taking the derivative of (7.68) and setting it equal to zero, that is:

$$\begin{aligned}
&\frac{d}{dt}r^2(t) = 0 \\
&\frac{d}{dt}r^2(t) = -2\pi A^2 F_1 \sin(4\pi F_1 t) - 2\pi B^2 F_2 \sin(4\pi F_2 t) - 2\pi AB(F_1 - F_2) \\
&\qquad \sin(2\pi(F_1 - F_2)t) - 2\pi AB(F_1 + F_2)\sin(2\pi(F_1 + F_2)t) = 0
\end{aligned} \tag{7.69}$$

The relationship in (7.69) occurs for $t = 2n\pi$, $n = 0, 1, \ldots$, that is:

$$P_{peak} = \max\left\{r^2(t)\right\} = r^2(0) = (A + B)^2 \tag{7.70}$$

The absolute value in (7.70) was dropped since $r(t)$ in this case is a real valued continuous function. Next, the average power of $r(t)$ is found as:

$$\begin{aligned}
P_{avg} &= MF_1 \int_0^{1/MF_1} \left[A\cos(2\pi F_1 t) + B\cos(2\pi MF_1 t)\right]^2 dt \\
&= \frac{A^2}{2} + \frac{B^2}{2} + \frac{A^2 MF_1}{2} \underbrace{\int_0^{1/MF_1} \cos(2\pi F_1 t)dt}_{0} + \frac{B^2 MF_1}{2} \underbrace{\int_0^{1/MF_1} \cos(2\pi MF_1 t)}_{0} \\
&\quad + AB \underbrace{\int_0^{MF_1} \cos(2\pi(F_1 - F_2)t)dt}_{0} + \underbrace{\int_0^{MF_1} AB\cos(2\pi(F_1 + F_2)t)dt}_{0} \\
&= \frac{A^2}{2} + \frac{B^2}{2}
\end{aligned} \tag{7.71}$$

The PAR is then the ratio:

$$PAR = 10\log_{10}\left(\frac{P_{peak}}{P_s}\right) = 10\log_{10}\left(\frac{\left(A + B\right)^2}{\frac{1}{2}\left(A^2 + B^2\right)}\right) = 10\log_{10}\left(2 + \frac{4AB}{A^2 + B^2}\right) \tag{7.72}$$

At this point it is instructive to look at two different cases. The first is when the two tones are of equal power, that is $A = B$. The relationship in (7.72) then becomes:

$$PAR = 10\log_{10}\left(\frac{P_{peak}}{P_s}\right) = 10\log_{10}\left(2 + \frac{4AB}{A^2 + B^2}\right)$$
$$= 10\log_{10}\left(2 + \frac{4A^2}{2A^2}\right) = 10\log(4) \approx 6dB \tag{7.73}$$

In (7.73), the result can be generalized to say that if the signal is made up of N tones that are of equal amplitude and that their phases are coherent in the sense that they add up constructively once over a certain period, then the PAR of this N-tone signal can be estimated as:

$$PAR = 20\log_{10}(N) \tag{7.74}$$

Note that, in reality, given an OFDM signal, for example, which is made up of N tones, the result presented in (7.74) is most unlikely to occur in the statistical sense due to the random nature of the data.

Next, we consider the case in which one tone is amplitude dominant over the other tone, say $A \gg B$. In this case, the relationship in (7.72) can be approximated as:

$$PAR = 10\log_{10}\left(\frac{P_{peak}}{P_s}\right) = 10\log_{10}\left(\frac{(A+B)^2}{\frac{1}{2}(A^2 + B^2)}\right)\Bigg|_{A+B\approx A \text{ since } A>>B}$$
$$= 10\log_{10}(2) \approx 3dB \tag{7.75}$$

The result in (7.75) implies that the PAR value is mostly influenced by the amplitude of the tones. If one of the tones is dominant, for example, then the resulting PAR is that of a single tone. In reality, in a multi-tone signal, the results are somewhere in between.

7.3.4.3 PAR of an IF-Signal

In this section, we discuss the signal PAR sampled at IF. It is imperative to note that in the ensuing analysis it is assumed that the IF frequency is much larger than the signal bandwidth. In certain waveforms such as OFDM UWB, the analysis may not apply.

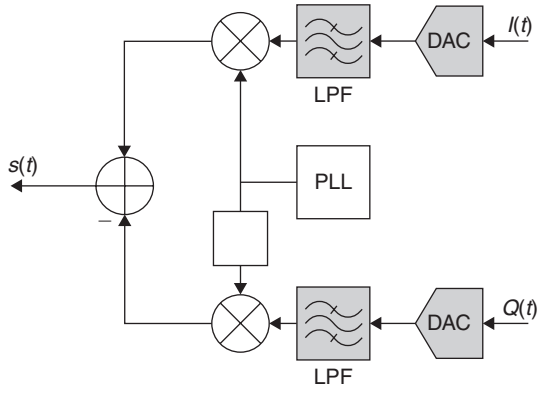

Figure 7.15 Quadrature signal modulator

Consider the IF signal $s(t)$ which is a byproduct of the in-phase and quadrature baseband signals $I(t)$ and $Q(t)$ as shown in Figure 7.15. To simplify the analysis, we ignore the effect of the lowpass filters digital or analog on the signal. The IF signal is given as:

$$s(t) = I(t)\cos(\omega t) - Q(t)\sin(\omega t) \tag{7.76}$$

The expression in (7.76) can be further expressed as the real part of $I(t) + jQ(t)$ modulated by the frequency ω, that is:

$$s(t) = \mathrm{Re}\left\{\left[I(t) + jQ(t)\right]e^{j\omega t}\right\} \tag{7.77}$$

The quadrature components of $s(t)$ can be written in terms of the envelope $r(t)$ and the phase $\theta(t)$, namely:

$$s(t) = r(t)\cos(\omega t + \theta(t)) \tag{7.78}$$

where the in-phase signal is:

$$I(t) = r(t)\cos(\theta(t)) \tag{7.79}$$

and the quadrature signal:

$$Q(t) = r(t)\sin(\theta(t)) \tag{7.80}$$

The relationships in (7.79) and (7.80) simply imply:

$$I^2(t) + Q^2(t) = r^2(t)\left\{\cos^2(\theta(t)) + \sin^2(\theta(t))\right\} = r^2(t) \tag{7.81}$$

or simply:

$$r(t) = \sqrt{I^2(t) + Q^2(t)} \tag{7.82}$$

Next denote the PAR of the baseband signal as the peak of power of the envelope signal $r(t)$ divided by the average power of $r(t)$ say:

$$PAR(r) = 10\log_{10}\left(\frac{P_{peak,r}}{P_{avg,r}}\right) = 10\log_{10}\left(\frac{\max\left|r(t)\right|^2}{E\left\{\left|r(t)\right|^2\right\}}\right) \tag{7.83}$$

where again the operator $E\{.\}$ is the expected value operator and $r(t)$ is real-valued. Next, we compare the PAR of the envelope signal at baseband $r(t)$ to the PAR of the IF signal $s(t)$. The PAR of $s(t)$ is:

$$PAR(s) = 10\log_{10}\left(\frac{\max\left|s(t)\right|^2}{E\left\{\left|s(t)\right|^2\right\}}\right) = 10\log_{10}\left(\frac{\max\left|r(t)\cos(\omega t + \theta(t))\right|^2}{E\left\{\left|r(t)\cos(\omega t + \theta(t))\right|^2\right\}}\right) \tag{7.84}$$

The numerator of (7.84) is simply $P_{peak,r}$ since the maximum of the cosine function is 1. Recall that the assumption again is that the signal bandwidth is much smaller than the IF frequency, and therefore the signal can be considered to be constant over many periods

of the modulating cosine function. Next, consider the denominator of (7.84). The average power of the signal $s(t)$ is[1]:

$$\begin{aligned} E\left\{\left|r(t)\cos\left(\omega t+\theta(t)\right)\right|^2\right\} &= \frac{1}{MT}\int_{t_0}^{\substack{t_0+MT\\M>>1}} s^2(t)\,dt \\ &= \frac{1}{MT}\int_{t_0}^{\substack{t_0+MT\\M>>1}} r^2(t)\cos^2\left(\omega t+\theta(t)\right)dt \\ &= \frac{1}{2MT}\left\{\int_{t_0}^{\substack{t_0+MT\\M>>1}} r^2(t)dt+\int_{t_0}^{\substack{t_0+MT\\M>>1}} r^2(t)\cos(2\omega t+2\theta(t))dt\right\} \\ &= \frac{P_{avg,r}}{2}+\frac{1}{2MT}\left\{\int_{t_0}^{\substack{t_0+MT\\M>>1}} \boldsymbol{r}^2(t)\cos(2\omega t+2\theta(t))dt\right\} \end{aligned} \tag{7.85}$$

Assume that the signal $r(t)$ is slowly varying over MT periods of the modulating cosine function and hence it can be taken outside the integral in (7.85). Then:

$$\int_{t_0}^{\substack{t_0+MT\\M>>1}} r^2(t)\cos(2\omega t+2\theta(t))dt \approx \hat{r}\int_{t_0}^{\substack{t_0+MT\\M>>1}} \cos(2\omega t+2\theta(t))dt = 0 \tag{7.86}$$

where $\hat{r}$ is a constant. Hence, the PAR of the IF signal in (7.84) can be finally defined as:

$$PAR(s) = 10\log_{10}\left(\frac{2P_{peak,r}}{P_{avg,r}}\right) = PAR(r)+3\text{ dB} \tag{7.87}$$

Hence it is obvious from (7.87) that the PAR of the baseband envelope signal is 3 dB less than that of the IF signal.

Another interesting facet of this discussion is to relate the PAR of the individual in-phase and quadrature components to the PAR of the envelope signal $r(t)$. If we consider $I(t)$

[1]Recall that $\cos^2 a = \left(1+\cos 2a\right)/2$.

and $Q(t)$ to be zero mean statistically independent Gaussian random variables, or more realistically if the desired in-phase and quadrature signals resemble Gaussian independent random variables, with zero mean and σ^2 variance, then the square of the envelope $r^2(t)$ is chi-square distributed and consequently $r(t)$ is Rayleigh distributed with a pdf of:

$$P_r(r(t)) = \frac{r(t)}{\sigma^2} e^{-r^2(t)/2\sigma^2},\ r(t) \geq 0 \tag{7.88}$$

The moments $r(t)$ are related to the gamma function as:

$$E\left\{r^n(t)\right\} = (2\sigma^2)^{n/2}\Gamma\left(1+\frac{n}{2}\right) \tag{7.89}$$

where:

$$\begin{aligned}
&\Gamma(v) = \int_0^\infty x^{v-1}e^{-x}dx,\ v > 0\\
&\Gamma\left(1+\frac{v}{2}\right) = \frac{1\times 3\times 5\times \ldots \times (2v-1)}{2^v}\sqrt{\pi}\\
&\Gamma(v) = (v-1)!,\ v \in \mathbb{N} \text{ and } v > 0\\
&\Gamma\left(\frac{3}{2}\right) = \frac{\sqrt{\pi}}{2}, \Gamma(2) = 1
\end{aligned} \tag{7.90}$$

This implies that the mean of the envelope $r(t)$ is:

$$E\left\{r(t)\right\} = \sqrt{\frac{\pi}{2}}\sigma \tag{7.91}$$

which is obviously nonzero compared to the zero mean of the in-phase and quadrature signal components. The variance of the envelope on the other hand is given as:

$$\sigma_r^2 = \left(2-\frac{\pi}{2}\right)\sigma^2 \tag{7.92}$$

The power of the envelope signal can be obtained via (7.89) as:

$$E\left\{r^2(t)\right\} = 2\sigma^2\Gamma(2) = 2\sigma^2 \tag{7.93}$$

Next, let us compare the PAR of say the in-phase signal to that of the envelope signal. Let the in-phase signal PAR be given as:

$$PAR(I) = 10\log_{10}\left(\frac{\max\left|I(t)\right|^2}{E\left\{\left|I(t)\right|^2\right\}}\right) = 10\log_{10}\left(\frac{M}{\sigma^2}\right) \tag{7.94}$$

and let the PAR of the envelope signal be:

$$PAR(r) = 10\log_{10}\left(\frac{\max\left|r(t)\right|^2}{E\left\{\left|r(t)\right|^2\right\}}\right) = 10\log_{10}\left(\frac{\max\left|\sqrt{I^2(t)+Q^2(t)}\right|^2}{2\sigma^2}\right) \tag{7.95}$$

Let $\max\left|\sqrt{I^2(t)+Q^2(t)}\right|^2 = M+\delta, \delta > 0$; then in order for the PAR of the envelope to be greater than the PAR of the in-phase component, it implies that:

$$\frac{M+\delta}{2\sigma^2} > \frac{M}{\sigma^2} \Rightarrow \delta > M \tag{7.96}$$

which is not likely for two Gaussian variables to have both maxima occur at the same instant. In fact, in an experiment of 2000 computations of the PAR of the in-phase, quadrature, and envelope signals comprised of 10,000 samples each, it was found that the relationship in (7.96) was true only a handful of times as shown in Figure 7.16. The in-phase and quadrature signals, in this case, are white Gaussian distributed with approximately zero-mean and unity variance. Figure 7.16 depicts the difference of $PAR(r)$ and $PAR(I)$, and $PAR(r)$ and $PAR(Q)$. Statistically, it can be observed that $PAR(I)$ and $PAR(Q)$ can be 3-dB or higher than $PAR(r)$. This is important to note since the AGC algorithm adjusts the gain line-up of the receiver based on the desired power of the envelope signal. And hence, the back-off from full scale takes into account the PAR of the envelope signal as seen previously and not the PARs of the in-phase and quadrature signals. However, in reality, that is not sufficient and care must be taken as to not clip the signal at the input of the converters in a non-IF sampling receiver. That is, the PAR of the in-phase and quadrature signals with respect to ADC full scale must be taken into account when setting the desired signal power in AGC algorithm.

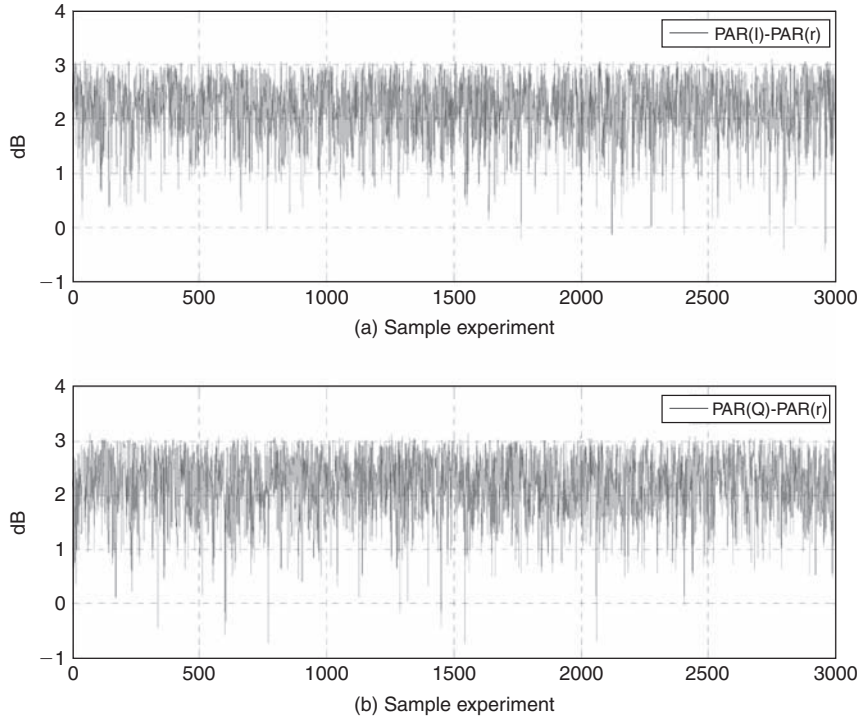

Figure 7.16 Difference in PAR between (a) in-phase signal and envelope signal and (b) quadrature signal

7.4 Appendix

7.4.1 Derivation of Analog Reconstruction Formula for Half Integer Positioning

In order to further simplify (7.36), recall that the RF or IF frequency can be expressed in terms of the bandwidth B as $F_c = (l - 1/2)B$, and that:

$$\begin{aligned}\cos(2\pi F_c t - 4\pi m F_c T_s) &= \cos(2\pi F_c t)\cos(4\pi m F_c T_s) + \sin E(2\pi F_c t)\sin(4\pi m F_c T_s) \\ &= \cos(2\pi F_c t)\cos\left(2\pi m\left(l - \frac{1}{2}\right)T_s\right) \\ &\quad + \sin(2\pi F_c t)\sin\left(2\pi m\left(l - \frac{1}{2}\right)T_s\right) \\ &= \cos(2\pi F_c t)\cos(-\pi m) = (-1)^m \cos(2\pi F_c t) \end{aligned} \tag{7.97}$$

Furthermore, consider the relation:

$$\begin{aligned}\cos(2\pi F_c t - 4\pi m F_c T_s + 2\pi F_c T_s) &= \cos(2\pi F_c t)\underbrace{\cos\left(2\pi\left(l-\frac{1}{2}\right)m - \pi\left(l-\frac{1}{2}\right)\right)}_{=0} + \\ &\quad \sin(2\pi F_c t)\sin\left(2\pi\left(l-\frac{1}{2}\right)m - \pi\left(l-\frac{1}{2}\right)\right) \\ &= \sin(2\pi F_c t)\sin\left(2\pi\left(l-\frac{1}{2}\right)m - \pi\left(l-\frac{1}{2}\right)\right) \\ &= \cos((m+l)\pi)\sin(2\pi F_c t) = (-1)^{m+l}\sin(2\pi F_c t)\end{aligned} \tag{7.98}$$

Substituting the results shown in (7.97) and (7.98) into (7.36) leads directly into the relationship established in (7.37).

References

[1] Vaughn R, et al. The theory of bandpass sampling. IEEE Trans. on Signal Processing, September 1991;39(9).
[2] Liu J, Zhou X, Peng Y. Spectral arrangements and other topics in first order bandpass sampling theory. IEEE Trans. on Signal Processing, June 2001;49(6):1260–3.
[3] Choe M, Kang H, Kim K. Tolerable range of uniform bandpass sampling for software defined radio. 5th International Symposium on Wireless Personal Multimedia Communications, Volume 2, Issue 27, 30 Oct. 2002, Page(s): 840–842.
[4] Qi R, Coakly FP, Evans BG. Practical consideration for bandpass sampling. IEEE Trans. on Electronics Letters, Sept 1996;32(20):1861–2.
[5] Proakis J. Digital Communications. 2nd Edition. New York, NY: McGraw-Hill; 1989.